Multi-objective optimization of small scale organic Rankine cycles for domestic solar applications

Barbazza, Luca; Pierobon, Leonardo; Haglind, Fredrik; Mirandola, Alberto

Published in:
8th Conference on Sustainable Development of Energy, Water, and Environment System

Publication date:
2013

Multi-objective optimization of small scale organic Rankine cycles for domestic solar applications

Luca Barbazza
Technical University of Denmark, Department of Mechanical Engineering,
Building 403, DK-2800 Kgs. Lyngby, Denmark
e-mail: barbazza.luca88@alice.it

Leonardo Pierobon[a], Fredrik Haglind[a], Alberto Mirandola[b]
[a]Technical University of Denmark, Department of Mechanical Engineering,
Building 403, DK-2800 Kgs. Lyngby, Denmark
[b]University of Padova, Department of Industrial Engineering,
via Venezia 1, 35131, Padova

ABSTRACT

Organic Rankine cycles can be utilized to convert the solar radiation harvested by solar collectors into electric power. In domestic applications, compactness, high performance and safe operation are crucial design aspects. Flat plate solar collectors can provide hot water at a temperature of 75°C while values higher than 120°C can be achieved by parabolic solar collectors. In the present work we design a small-scale organic Rankine cycle tailored for domestic solar applications where the net power output is between 3 kW_e and 6 kW_e. We employ a multi-objective genetic algorithm to optimize simultaneously the net power output of the organic Rankine cycle and the volume of the heat exchangers. We consider the evaporating pressure, the working fluid, the pinch point at the inlet of the evaporator, the pinch point of the condenser and the geometry of economizer, evaporator and condenser as optimization variables. Flat plate heat exchangers with herringbone corrugations are selected as heat transfer equipment for the economizer, the evaporator and the condenser. Findings suggest that the higher the net power output, the lower the compactness of the heat exchangers. The results also indicate that the working fluid, the evaporating pressure and the pinch point of the evaporator have the greatest impact on the performance of the cycle and on the compactness of the system.
Among the fluids considered, R1234yf and R1234ze are the best alternatives. Namely, with a hot water temperature of 75°C and a mass flow rate of the heat source of 1.2 kg/s, R1234yf is the optimal working fluid. The optimal volume of economizer, evaporator and condenser ranges between 6.0 and 23.0 dm^3 whereas the heat transfer area varies between 2.2 and 7.2 m^2 and the thermal efficiency is around 4.5%. R1234ze is the best working fluid with a hot water temperature of 120°C and a mass flow rate of the heat source of 0.4 kg/s. The thermal efficiency is around 6.9%. The volume of economizer, evaporator and condenser varies from 6.0 to 18.0 dm^3 and the heat transfer area ranges between 2.2 and 5.7 m^2.

1 INTRODUCTION

The exploitation of solar energy in domestic applications has received growing attention due to the increasing consumption of electric energy, the scarcity of fossil fuels (oil, natural gas and coal) and environmental concerns. In recent years, many researchers have attempted to utilize solar energy to cover part of the heat demand or to convert the heat directly into electricity. Organic Rankine cycles (ORCs) are a promising technology that can be utilized to convert the solar radiation harvested by solar collectors into electric power. This technology is in principle similar to the conventional steam power plants but it employs an organic working fluid instead of water to convert the thermal energy

into work. An ORC presents several advantages compared to steam plants. Major benefits are the simplicity of the cycle and the possibility of tailoring the working fluid to the specific temperature profile of the heat source. Furthermore, the ORC eliminates the problem of turbine blade erosion due to the liquid droplet formation by utilizing a “dry” fluid as the working fluid.

As surveyed by Tchanche et al. [1], the performance of the ORC is strongly related to the working fluid and the heat source temperature, therefore the selection of the optimal working fluid is a crucial research topic. For example, Tchanche et al. [1] investigated the thermodynamic characteristics and performances of 20 fluids for a small scale solar organic Rankine cycle and R134a was recommended as optimal working fluid. Quoilin et al. [2] studied the thermodynamic performance of a solar organic Rankine cycle and demonstrated that solkatherm was the most efficient fluid even though high expander volumes were obtained. Hettierachi et al. [3] presented the optimum design of an ORC system utilizing a low temperature geothermal heat source (70-90°C). The objective function was the total heat transfer area to the net power output and ammonia was suggested as working fluid among four possible alternatives. Pierobon et al. [4] carried out a multi-objective optimization of a waste heat recovery system for offshore application using ORC technology. Genetic algorithm was employed to design the system and thermal efficiency, compactness and net present value were the objective functions. The results suggested that acetone and cyclopentane were the most suitable working fluids.
Wang et al. [5] analyzed the influence of the inlet temperature of the heat source and of the pinch point of the evaporator on the performance and on the economic characteristics of the ORC. The results revealed that R123 was the best working fluid for a temperature range of the hot source from 100°C to 180°C while R141b was the optimal choice when the temperature of the hot source was higher than 180°C. Lakew and Bolland [6] investigated the power production capability of simple ORCs driven by low-temperature (80-200°C) heat sources with different working fluids (R123, R245fa, R134a, R290, R227ea and n-pentane). The results indicated that R227ea and R245fa provided the highest power with a temperature of the heat source in the range of 80-160°C and of 160-200°C. Wang et al. [7] conducted a multi-objective optimization of an ORC system with evolutionary algorithm with two conflicting objective functions, namely, the exergy efficiency and the overall capital cost. The temperature of the exhaust gas was 130°C and R134a was selected as working fluid. The results revealed that the optimal turbine inlet pressure was in the range of 1.8-2.4 MPa whereas the optimal turbine inlet temperature was located around 90°C.

The present work aims at designing a small-scale organic Rankine cycle tailored for domestic solar applications. The requirements in domestic applications are high performance, compactness and safe operation. The multi-objective optimization modeled by the genetic algorithm is adopted to optimize simultaneously the net power output and the compactness of the ORC. We select a set of working fluids considering operating conditions, environmental impact, safety and commercial availability. The compactness of the ORC is assessed by calculating the sum of the volumes of the heat exchangers (economizer, evaporator and condenser). Flat plate heat exchangers are selected as heat transfer equipment and the geometry of the economizer, evaporator and condenser is included in the optimization routine by utilizing appropriate correlations for the heat transfer coefficient and the pressure drops. The design variables include the turbine inlet temperature, the outlet temperature of the condenser, the pinch point of the condenser, the pinch point of the evaporator (which is located at the inlet of the working fluid side) and the geometry of the heat transfer equipment. Compared with previous works [1-3,5,6,8], the approach in this paper is novel in the sense that it considers the net power output and the total volume as objective functions. Furthermore, in this work the geometry of the flat plate heat exchangers is included in the optimization procedure in order to assess the influence of the heat transfer equipment on the performance and compactness of the system. This methodology can be applied in domestic applications where the ORC design is the results of a compromise between high performance and compactness.

Two cases of study are considered. In the first the temperature and the mass flow of the hot source (liquid water) are 75°C and 1.2 kg/s while in the second the temperature is increased up to 120°C and the mass flow is 0.4 kg/s. The temperatures of heat source are the common values provided by flat plate solar collectors and parabolic solar collectors while the mass flow rates are chosen considering an expected value of the net power output between 3 kW_e and 6 kW_e.

We describe the methodology utilized in this paper in section 2. In this section we also present the two cases of study and the algorithm used to optimize the system. Results of the multi-objective optimization are reported in section 3 and discussed in detail in section 4. Finally, we state the main conclusions in section 5.

2 METHODOLOGY

The ORC system and the selection of the working fluid are described in section 2.1 and 2.2. The correlations used to calculate the heat transfer coefficient and the friction factor for plate heat exchangers are reported in section 2.3 whereas the multi-objective approach and the optimization procedure are outlined in section 2.4.

2.1 System description and selection of working fluid

A solar driven ORC system consists of a subsystem collecting the solar energy and an organic Rankine cycle. Two different types of solar collectors are considered: the flat plate solar collectors and the parabolic solar collectors. Flat plate solar collectors provide hot water at a temperature up to 80°C whereas temperatures higher than 120°C can be obtained by parabolic solar collectors.

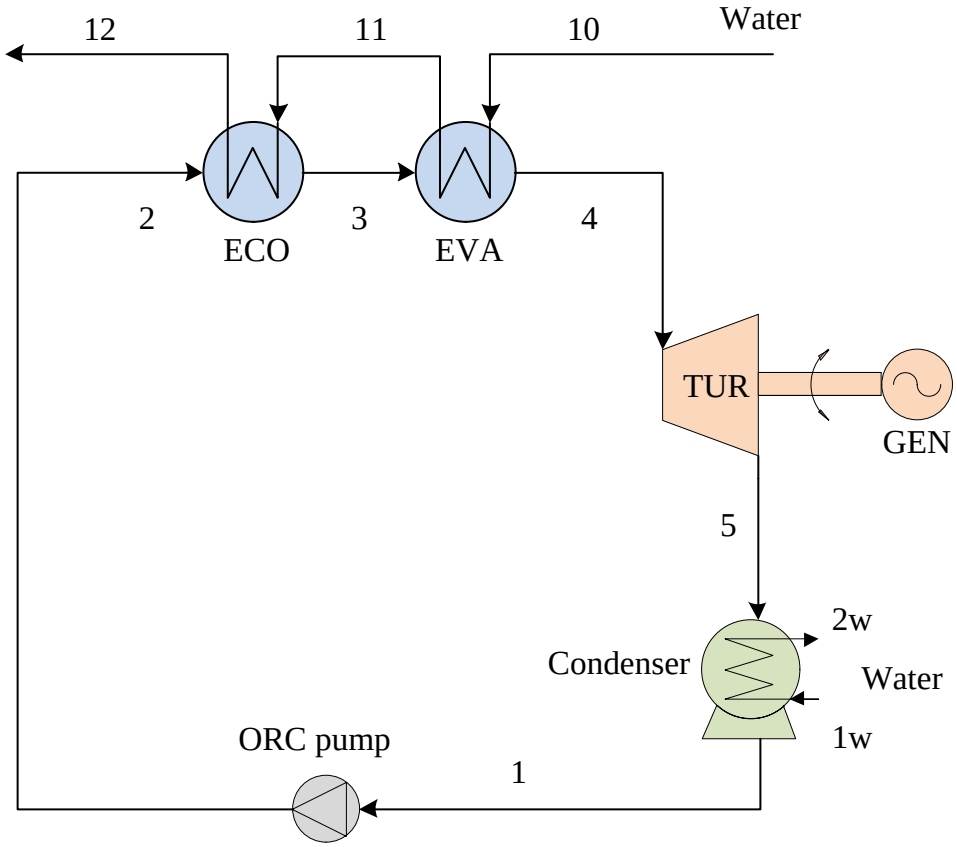

Figure 1. Layout of the solar – driven ORC system. The hot source is liquid water coming from the solar collectors.

As shown in Figure 1, the organic Rankine cycle consists of five components: a pump, an economizer, an evaporator, an expander and a condenser. The pump pressurizes the liquid fluid which is injected into the economizer and the evaporator to produce vapor that is expanded in a turbine connected to an electric generator. The economizer and the evaporator are the devices that allow the heat transfer between the heat source and the working fluid. Finally, the vapor discharged at the outlet of the expander is condensed and sucked up by the pump to complete the cycle.

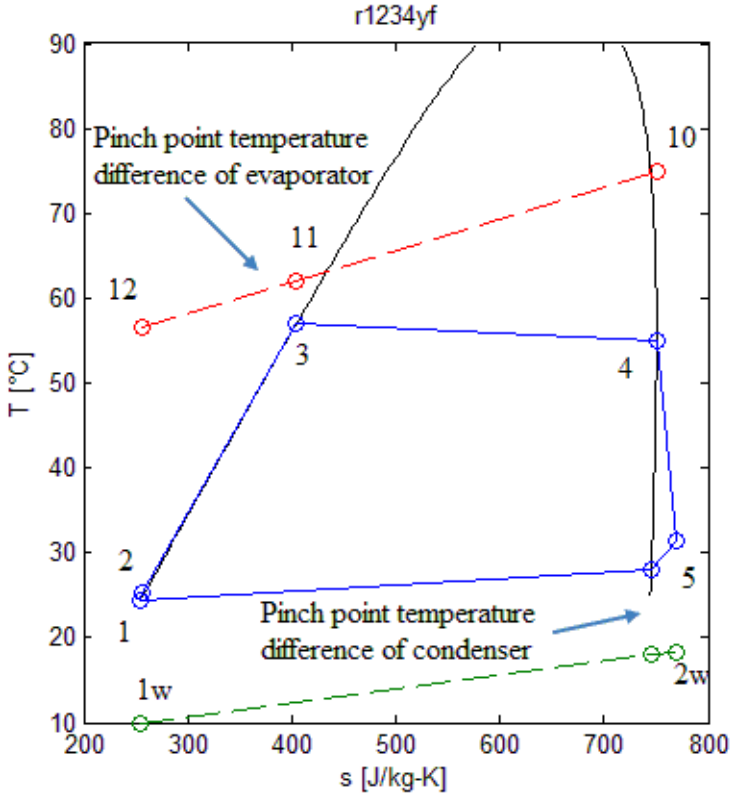

Figure 2. T-s diagram of a conventional solar-driven ORC system.

Figure 2 illustrates a typical T-s diagram of the solar driven regenerative ORC system. The temperature profile of the heat source and the temperature profile of the cooling water are also depicted. In this case the minimum temperature difference of the heating process is located at the inlet of the evaporator. The selection of the working fluids plays a key role in the ORC power plant design [8] and several criteria have to be satisfied. Namely, the working fluid should match with the temperature range of the specific application; moreover, it should be economical, nontoxic and inflammable. The thermo-physical properties of the working fluid that mostly affect the performance of the system are the density, the specific heat, the thermal conductivity and the specific volume at saturation conditions (condensing process). Furthermore, the growing attention to environmental impact limits the list to fluids under investigation as they should present a low ozone depleting potential (ODP) and global warming potential (GWP). In this work, we consider five fluids: R1234yf, R1234ze, R245fa, R245ca and n-pentane. The fluid R134a is not considered since it will be replaced by R1234yf and R1234ye as refrigerant in the next years. Refrigerants such as R123, R141b and R142b are excluded from the selection process due to their high global warming potential. According to Quoilin [2], Lakew and Bolland [6] and Wei [12], R245fa, R245ca and n-pentane are suitable alternatives for small and medium scale applications and are, therefore, selected together with R1234yf and R1234ze as possible working fluids. Table 1 lists the thermo-physical properties, the environmental impact and the hazard properties of the each fluid. None of the candidates affect the ozone layer since the ODP value is zero, whereas R1234yf and R1234ze have the lowest global warming potential. Among the fluids considered, n-pentane presents the highest flammability risk while R24fa, R245ca and n-pentane have the highest toxicity.

Table 1. Thermodynamic properties at the critical point, ozone depleting potential (ODP), global warming potential (GWP) and hazard properties based on the ASHRAE Standard 34 of the working fluids investigated.

Fluid	M [g·mol^{-1}]	T_{crit} [°C]	P_{crit} [bar]	ODP	GWP	ASHRAE 34
R1234yf	114.04	94.7	33.82	0	4	A2
R1234ze	114.04	109.4	36.36	0	6	A2
R245fa	134.05	154.0	36.51	0	950	B1
R245ca	134.05	174.4	39.25	0	560	B1
n-pentane	72.15	196.5	33.7	0	11	B3

ASHRAE Standard 34 – Refrigerant safety group classification. 1: No flame propagation, 2: Lower flammability, 3: Higher Flammability, A: Lower toxicity; B: Higher toxicity.

2.2 Organic Rankine cycle modeling

In this section, we present the steady-state model of the system given in Figure 1. The model aims at calculating the thermodynamic variables, the net power output and the thermal efficiency of the ORC. The plant is modeled in Matlab 2012a [9] and the commercial software REFPROP 9.0 [10] is utilized to calculate the thermo-physical properties of the fluids. To solve the ORC, we make the following assumptions:

- Saturated vapor and saturated liquid are assumed at the turbine inlet and at the condenser exit respectively
- All components except for the electric generator are considered adiabatic

Table 2. Parameters assumed to model the organic Rankine cycle for case 1 and case 2.

Variable	Case 1	Case 2
Heat source inlet temperature [°C]	75	120
Cooling water inlet temperature [°C]	10	10
Mass flow rate of heat source [kg/s]	1.2	0.4
Pressure of the heat source (water) [bar]	1.0	3.0
Expander isentropic efficiency [%]	60	60
Pump isentropic efficiency [%]	70	70
Electric generator efficiency [%]	98	98

The cycle specifications for the cases of study considered are listed in Table 2. The optimization variables of the Rankine cycle are the inlet temperature of the expander (T_4), the outlet temperature of the condenser (T_1), the ORC working fluid, the pinch point at the inlet of the evaporator (T_{ppe}) and the pinch point of the condenser (T_{ppc}).

Table 3. Parameters assumed to model the flat plate heat exchangers (the values are acquired from Ramesh et al. [13]).

Variable	Value
Plate thickness t [m]	0.0004
Plate thermal conductivity λ [W/mK]	15.4
Chevron angle β [°]	60
Compact aspect ratio [-]	1.0
Enlargement factor [-]	1.22
Fouling resistance R_f [m^{2}K/W]	0.5e-4

Flat plate heat exchangers with herringbone corrugations are selected for the economizer, evaporator and condenser. In order to model the heat transfer equipment, the following four design parameters are selected: the plate width, the number of channels per pass, the number of passes and the mean channel spacing. The main characteristics of the plates are listed in Table 3. For small scale and low temperature heat sources, flat plate heat exchangers are preferable compared to shell and tube heat exchangers due to their compactness and high heat transfer coefficients which imply less heat transfer area. Furthermore, flat plate heat exchangers are easier to maintain and have a lower tendency to fouling. The modeling of heat transfer equipment allows us to consider the pressure drops which affect the enthalpy drop in the expander.

$$\dot{W}_{net} = \eta_{el}\, \dot{m}\, (h_4 - h_5) - \dot{m}\, (h_2 - h_1) \tag{1}$$

As indicated in Eq. (1), the net power $\dot{W}_{net}$ is defined as the difference between the power of the turbine and the power consumption of the pump. The thermal efficiency of the ORC η_{ORC} can be expressed as follows:

$$\eta_{ORC} = \frac{\dot{W}_{net}}{\dot{m}(h_4 - h_2)} \tag{2}$$

2.3 Flat plate heat exchangers

We apply the logarithmic mean temperature method in order to calculate the heat transfer area required by the heat exchanger:

$$\dot{Q} = U\, A\, F_t\, \Delta T_{lm} \tag{3}$$

where $\dot{Q}$ is the heat rate, U is the overall heat transfer coefficient, A is the heat transfer area, ΔT_{lm} is the logarithm mean temperature difference and F_t is the temperature correction factor [14] which accounts for co-current and cross-flow. In the economizer the working fluid is in single-phase whereas in the evaporator and condenser a two-phase heat transfer occurs. The equations employed to evaluate the heat transfer coefficient in the single-phase and two-phase region (evaporation and condensation) as well as the friction factor are reported below.

In the single-phase regime we use the empirical correlations utilized in Ayub [15] to estimate the heat transfer coefficients and friction factors. The Nusselt number and the friction factor are functions of the Reynolds and Prandtl numbers, and the chevron angle of the plates:

$$Nu = 0.205 Pr^{1/3} \left(\frac{\mu}{\mu_w}\right)^{0.17} (f Re^2 \sin 2\beta)^{0.374} \tag{4}$$

$$\frac{1}{\sqrt{f}} = \frac{\cos\beta}{(0.045\tan\beta + 0.09\sin\beta + f_0/\cos\beta)^{0.5}} + \frac{1-\cos\beta}{\sqrt{3.8 f_1}} \tag{5}$$

For the evaporation process the correlations derived by Han et al. [16] are used:

$$Nu = Ge_1 {Re_{eq}}^{Ge_2} {Bo_{eq}}^{0.3} Pr^{0.4} \tag{6}$$

$$f = Ge_3 {Re_{eq}}^{Ge_4} \tag{7}$$

For the condensation the approach developed by Longo et al. [17] is adopted:

$$Nu = j Pr^{1/3} \tag{8}$$

$$j = \begin{cases} 60 & Re_{Eq} < 1750 \\ \frac{75-60}{3000-1750}\left(Re_{Eq} - 1750\right) + 60 & Re_{Eq} > 1750 \end{cases} \quad (9)$$

The pressure drops in the heat exchangers are computed as follows [13]:

$$\Delta p = 4f\frac{G^2 L_v N_{pass}}{2\rho D_e} \quad (10)$$

2.4 The multi-objective optimization

Finding the optimal working fluid, selecting the design variables of an ORC and sizing the heat transfer equipment require using an optimization routine. In the present paper, the multi-objective optimization modeled by the genetic algorithm is utilized due to the benefits of optimizing simultaneously two or more functions. Furthermore, the genetic algorithm avoids the calculation of complex derivatives and enables to search the global optima. In the genetic algorithm an initial population of strings is created and a single string stands as a possible solution to a specific task. Each solution is then assessed by means of an objective function. A portion of the initial population is maintained, based on certain operation probabilities for crossover and mutation to produce a new generation. Fitter strings replace the poorer strings in order to improve the overall fitness to the objective function. In the present paper the design variables considered are the temperature at the inlet of the expander (T_4), the pinch point temperature at the inlet of the evaporator (T_{ppe}), the fluid, the pinch point temperature of the condenser (T_{ppc}), the temperature at the inlet of the pump (T_1) and the parameters necessary to design the heat exchangers. In order to model the flat plate heat exchangers, four design variables are considered for each heat exchanger: plate length (L_w), number of channels per pass (N_{ch}), mean channel spacing (b) and number of passes (N_{pass}).
In the present case, the objective functions are the net power output of the organic Rankine cycle and the sum of the volumes of the heat exchangers. The two objective functions can be formulated mathematically as follows:

$$f_1 = -W_{net} \quad (11)$$

$$f_2 = V_{preh} + V_{eva} + V_{cond} \quad (12)$$

where volume V of each heat exchanger is computed as follows:

$$V = \left[2N_{ch}N_{pass}b + \left(2N_{ch}N_{pass} + 1\right)t\right]L_w L_v \quad (13)$$

In the case of a multi-objective optimization, the solution is not a single set of variables. The result is a number of possible solutions which cannot simply be compared with each other. For such solutions, called Pareto optimal solutions, no improvement is possible in any objective function without sacrificing at least one of the other objective functions. In order to produce consistent results for the design of the ORC, reasonable upper and lower boundaries are selected. The lower and upper values for each of the optimization variable and the constraints specified within the algorithm are listed in Table 4.
The multi-objective genetic algorithm utilized in this work is embedded in the MATLAB 2012a optimization toolbox. The routine is initialized by setting the ranges of variation of the design variables and the constraints listed in Table 4.

Table 4. Upper and lower bounds for each of the optimization variable and the constraints specified within the algorithm in the multi-objective optimization [18].

Variable	Lower value	Upper value
Design variables		
Temperature at the inlet of the expander [°C]	45	65/110
Pinch point at the inlet of the evaporator [°C]	5	15
Temperature at the inlet of the pump [°C]	20	35
Pinch point of the condenser [°C]	5	15
Width of plates [m]	0.080	0.200
Channel spacing [m]	2.0e-3	3.0e-3
Number of channels per pass	1	30
Number of passes	1	4
Constraints		
Ratio L_v/L_w	2	4
Fluid velocity inside the channels [m/s]	0.1	1.5
Temperature at the inlet of the turbine [°C]	-	$min[T_{crit}, T_7 - T_{ppe}]$
Temperature T_6 [°C]	$T_{10} + T_{ppc}$	-

An iterative procedure is necessary to calculate the operating points of heat exchangers, expander and pump. The first iteration aims at defining the operating points with the design variables selected by the algorithm. When the operating point is calculated, it is possible to size the heat transfer equipment that satisfies the required heat transfer rate. By modelling the heat exchangers, we can evaluate the pressure drops and subsequently use them to calculate the new operating point. Finally, the net power output and the volume of the heat exchangers are computed and evaluated as objective functions. This procedure is repeated until convergence is obtained.

3 RESULTS

The Pareto fronts obtained through the multi-objective optimization are shown in Figure 3. It can be noted that the trend of the volume vs. the net power output is hyperbolic. Namely, the higher the net power output the steeper the increment in the volume of the heat transfer equipment. Hence, the solution with the highest net power output corresponds to the highest dimensions of the economizer, evaporator and condenser. Similarly, on the leftmost point, the volume and the net power generated reach their minimum values. This behavior indicates that the solutions of the multi-objective optimization are a trade-off between the fitness functions considered. The first case of study represents the system where the temperature of the heat source at the inlet of the evaporator is 75°C and the mass flow rate is 1.2 kg/s (see Table 2). The multi-objective optimization gives a Pareto front where the net power output ranges between 2.0 kW and 4.5 kW while the volume varies from 6.0 dm^3 to 23.0 dm^3. In this case the optimal working fluid is R1234yf with an optimal evaporating temperature of around 57°C. The pressure of the fluid at the inlet of the expander is around 15.2 bar while the temperature and the pressure at the outlet of the condenser are 22°C and 6.3 bar respectively. The thermal efficiency of the ORC presents a minimum value of 4.3% and a maximum value of 4.7%

The same trend is found for a heat source with an inlet temperature of 120°C and a mass flow rate of 0.4 kg/s. However, in this simulation R1234ze is the optimal fluid. The net power output generated by the system varies between 4.0 kW and 6.3 kW whereas the volume of the heat transfer equipment ranges between 6 dm^3 and 20 dm^3. It can be noted that the optimal evaporation temperature varies between 83.0°C and 89.0°C which correspond to an evaporation pressure between 21.4 bar and 24.2 bar. The temperature at the outlet of the condenser is around 24°C while the pressure is approximately 5 bar. The minimum value of the thermal efficiency is 6.8% while the

maximum value is 7.1%. In comparison with the results of the optimization of the first case of study, the Pareto front of the second case is shifted to higher power output. This result is due to the higher enthalpy drop caused by the higher temperature difference between the hot and the cold sources. The space requirements are about the same. The higher heat source temperature of the second case of study affects also the value of the thermal efficiency. In fact, the second case presents a thermal efficiency around 7% that is 2.5%-points higher than that of the first simulation where the heat source temperature is 75°C. The evaporating pressure of the second case of study is in the range of 21.0-24.0 bar. On the contrary, the pressure level of the second case is found to be higher than the optimal value of 15 bar of the first case of study. Compared to an optimal condensing pressure of 6 bar for the first case of study, the condensing pressure of the second case is lower (4.8-5.0 bar).

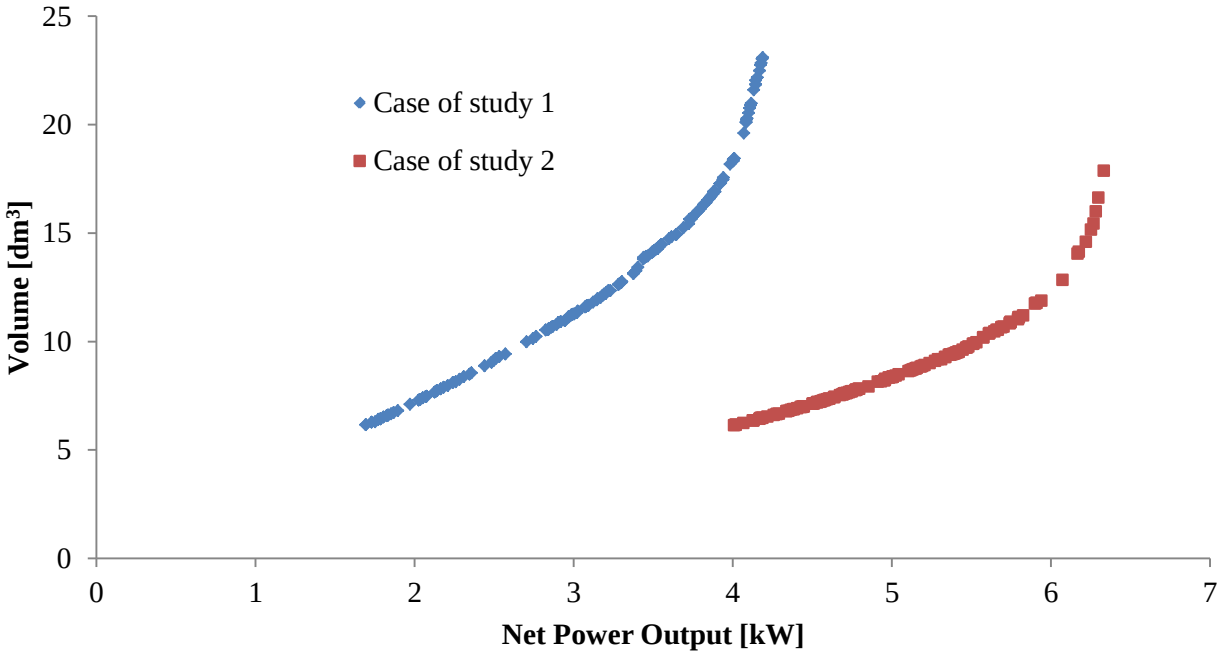

Figure 3. Pareto fronts for the two cases of study listed in Table 2.

Figures 4 and 5 depict the effect of the pinch point at the inlet of the evaporator and the pinch point in the condenser on the net power output and on the volume for the two cases of study. It can be noted that this design variable has a great impact on both the net power output and volume. In fact, decreasing the pinch point at the inlet of the evaporator enhances the power production of the ORC since of the thermodynamic irreversibility associated with the heat transfer is diminished. On the other hand, solutions with a higher pinch point improve the compactness of the ORC even though lower performances are obtained.

Figure 6 shows the relative contribution of each heat exchanger to the total volume. It can be noted that the volume of the condenser is about the 60% of the total volume. Hence, the condenser is the largest heat exchanger with a volume that ranges between 4.0 and 15.0 dm^3. This can be explained with the poor performance of the ORC. In fact, the low thermal efficiency of the ORC results in a high amount of heat rejected through the condenser which in turns needs to be larger compared to the economizer and the evaporator. Furthermore, the values of overall heat transfer coefficient and logarithmic mean temperature difference for the condenser are around 1900 W/m^2K and 11°C. On the contrary, higher values are encountered for the economizer (2000 W/m^2K and 20°C) and for the evaporator (2600 W/m^2K and 14°C).

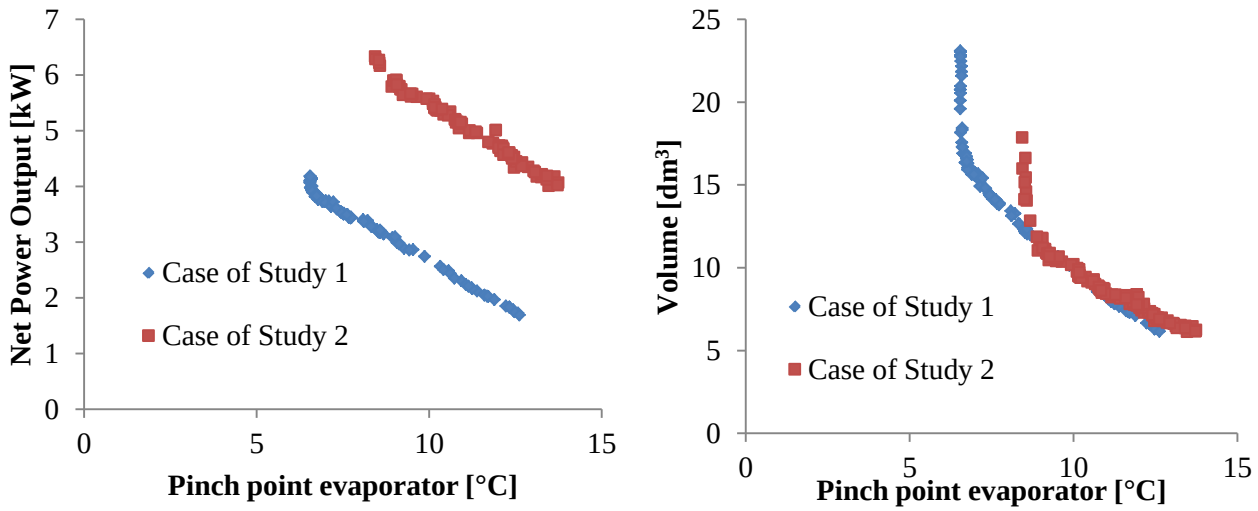

Figure 4. a) Net power output of the organic Rankine cycle vs. pinch point at the inlet of the evaporator for the two cases of study listed in Table 2; b) Volume of the heat transfer equipment vs. pinch point at the inlet of the evaporator.

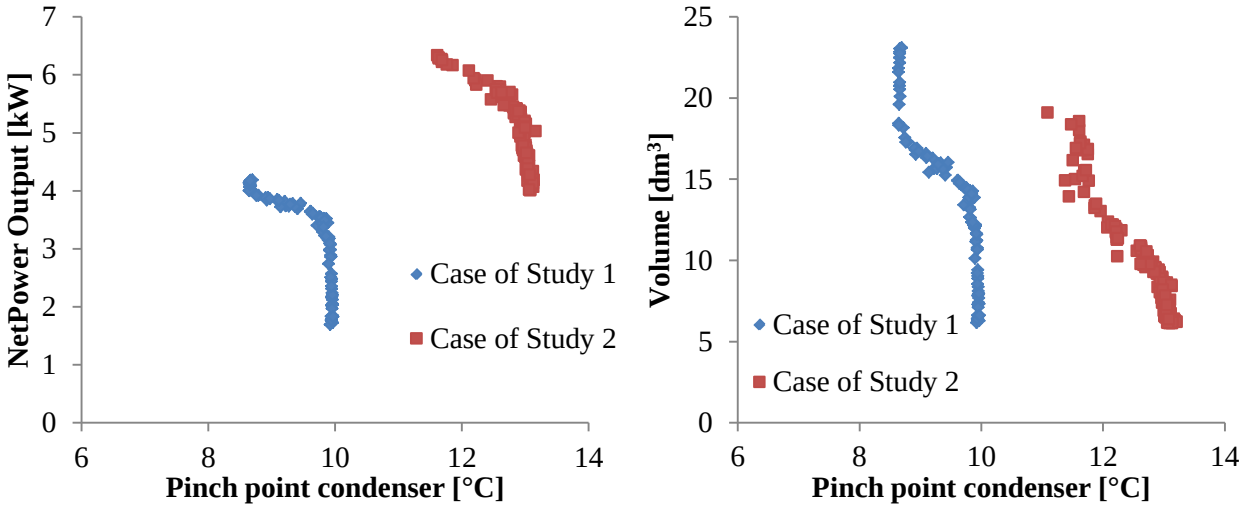

Figure 5. a) Net power output of the organic Rankine cycle vs. pinch point of the condenser for the two case of study listed in Table 2; b) Volume of the heat transfer equipment vs. pinch point of the condenser.

4 DISCUSSION

The Pareto fronts shown in Figure 3 can be utilized in the design of the organic Rankine cycle to select the solution that fits better with the specific design requirements. For example, if the volume of the heat exchangers must be limited to 13 dm^3, the net power produced by the ORC is around 3.3 kW for the first case of study and 6.0 kW for the second.

Table 5. Design variables of the ORC and geometry of the economizer, evaporator and condenser for two possible solutions selected from the Pareto front.

Variable			**Case of study 1**			**Case of study 2**
Net power output [kW]			3.3			6.0
Total volume [dm^3]			12.79			12.83
Working fluid			R1234yf			R1234ze
Mass flow rate [kg/s]			0.443			0.449
Temperature T_4 [°C]			56.6			83.4
P_4 [bar]			15.2			21.6
Pinch Point evaporator [°C]			8.3			8.7
T_1 [°C]			22.2			23.7
P_1 [bar]			6.3			4.8
Pinch Point condenser [°C]			9.9			12.1
ORC efficiency [%]			4.5			7.0
	Eco	**Eva**	**Cond**	**Eco**	**Eva**	**Cond**
U [W/m^2K]	2102	2526	1811	1865	2829	1827
A^a [m^2]	0.445	1.589	2.886	0.890	0.704	2.450
L_w [m]	0.119	0.113	0.190	0.144	0.163	0.169
L_v [m]	0.338	0.371	0.420	0.561	0.355	0.341
b [mm]	2.22	2.24	2.25	2.30	2.30	2.40
N_{pass}	1	2	1	1	1	1
N_{ch}	6	16	19	6	6	25
ΔP [kPa][b]	8.4	2.1	46.9	6.7	1.8	46.0

[a]Projected Area; [b]Working fluid side.

The design variable of the ORC and the geometry of the economizer, evaporator and condenser for the two possible solutions corresponding to a volume of 13 dm^3 are listed in Table 5. The plate width, the channel spacing and the number of channels per pass are reported. Table 5 includes also the pressure drops obtained for each heat exchanger. It is worthwhile noticing that the pressure drop through the evaporator converges to a relatively low value (0.132% of evaporating pressure). The main reason is that by decreasing the evaporation pressure, the turbine inlet temperature is affected causing a drop of the net power output.

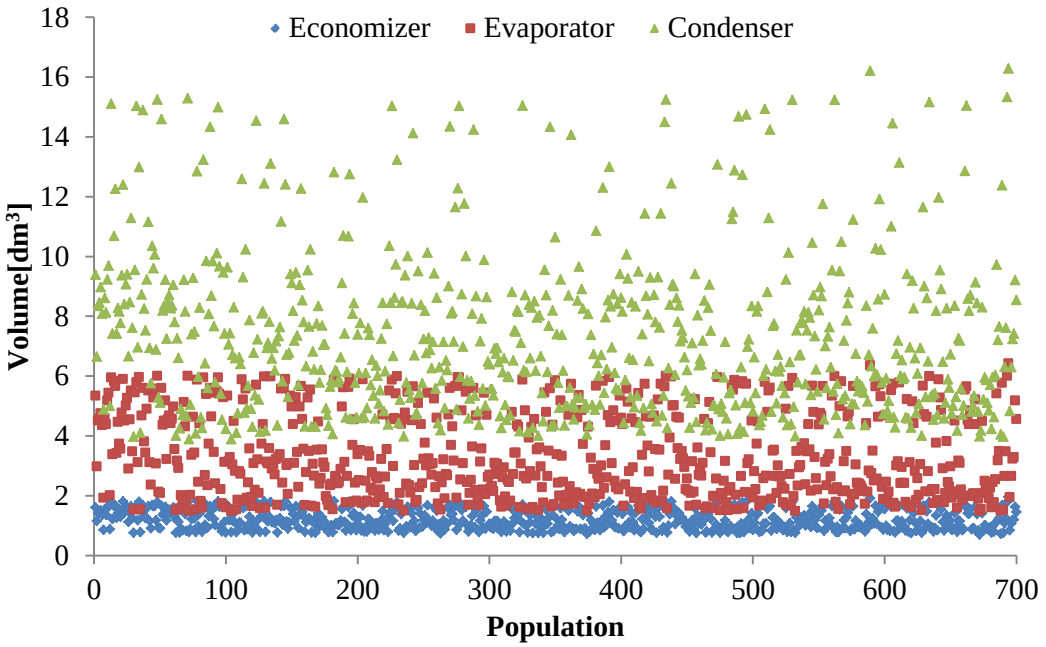

Figure 6. Volume of economizer, evaporator and condenser obtained through the multi-objective optimization for each point of the Pareto front.

In the economizer, the pressure drop has a lower impact since the fluid is in liquid phase and the enthalpy is only slightly influenced by the pressure (incompressible fluid). On the contrary, since the amount of heat transferred is higher in the condenser than those of the economizer and the evaporator, a higher pressure drop (7.3% of condensing pressure) is accepted in the condenser. In fact, this enables to increase the velocity and consequently the heat transfer coefficient of the working fluid in the condenser. Hence, a lower heat transfer area is obtained even if the power output of the expander is reduced.

5 CONCLUSION

In this study we employ a multi-objective optimization modeled with the genetic algorithm to find the optimal design of a solar-driven organic Rankine cycle for domestic applications. Due to the particular case of study, the major requirements of such system are high performance, compactness and safe operation. Thus, a multi-objective algorithm employing the net power output of the ORC and the sum of the volume of the economizer, evaporator and condenser as objective functions is utilized to design the system. Considering the hot source temperature and the size of the system, the heat transfer equipment is the flat plate heat exchanger. The economizer, evaporator and condenser are modeled with specific correlations evaluating the heat transfer coefficient and the pressure drops. We investigated two boundary conditions for the hot source (liquid water). Namely, inlet temperature of 75°C and mass flow rate of 1.2 kg/s for the first case and inlet temperature of 120°C and mass flow rate of 0.4 for the second. The results indicate that the optimal working fluid is R1234yf with an inlet temperature of the hot source of 75°C and R1234ze for an inlet temperature of the hot source of 120°C. The results of the multi-objective optimization reveal a hyperbolic relationship between the net power output of the system and the volume of the heat exchangers. Among the design variables considered in the optimization process, the pinch point at the inlet of the evaporator has the greatest influence on the net power production and on the volume of the heat exchangers. The power output increases with the decrease of pinch point temperature difference in the evaporator whereas the volume decreases with the increase of this temperature difference. The methodology presented in this paper can be employed to select the most suitable design of solar-driven ORCs by specifying the desired volume of the economizer, evaporator and condenser. By introducing the volume in the Pareto front, the geometry of the heat transfer equipment and the design variables of the ORC can be identified.

Nomenclature

Annotations

A	Area [m^2]
b	Mean channel spacing [m]
c	Specific heat [J/(kg K)]
D_e	Equivalent diameter [m]
f	Friction factor [-]
G	Specific mass flow rate [kg/(m^2 s)]
h	Specific enthalpy [J/(kg K)]
j	Colburn factor [-]
k	Heat transfer conductivity [W/(m K)]
L_v	Plate length [m]
L_w	Plate width [m]
$\dot{m}$	Mass flow rate [kg/s]
N_{ch}	Number of channels per pass
N_{pass}	Number of passes
p	Pressure [Pa]
Pr	Prandtl number [-]
$\dot{Q}$	Heat transfer rate [W]
Re	Reynolds number
R_f	Fouling resistance [m^2 K/W]
T	Temperature [K]
t	Plate thickness [m]
U	Overall heat transfer coefficient [W/(m^2 K)]
u	Velocity [m^2/s]
V	Volume [m^3]
$\dot{W}$	Power [W]

Greek symbols

α	Heat transfer coefficient [W/(m^2 K)]
β	Chevron angle [°]
μ	Viscosity [Pa s]
ρ	Density [kg/m^3]
η_{el}	Electric generator efficiency [%]
η_{ORC}	ORC Efficiency [%]
λ	Heat transfer conductivity of plate [W/(mK)]
ΔT_{lm}	Logarithmic mean temperature difference

Subscripts and superscripts

cond	Condenser
c	Cold fluid
eco	Economizer
eva	Evaporator
h	Hot fluid
hs	Heat source
in	Inlet
out	Outlet
ppc	Pinch point of condenser
ppe	Pinch point of evaporator
wf	Working fluid
wtr	Cooling Water

References

[1] Tchanche B, Papadakis G, Lambrinos G, Frangoudakis A. Fluid selection for a low-temperature solar organic Rankine cycle. Applied Thermal Engineering 2009;29:2468-2476.

[2] Quoilin S, Orosz M, Hemond H, Lemort V. Performance and design optimization of a low-cost solar organic Rankine cycle for remote power generation. Solar Energy 85;2011:955-966.

[3] Hettiarachchi H, Golubovic M, Worek W, Ikegami Y. Optimum design criteria for an Organic Rankine cycle using low-temperature geothermal heat sources. Energy 32; 2007:1698-1706.

[4] Pierobon L, Nguyen TV, Larsen U, Haglind F, Elmegaard B. Multi-objective optimization of organic Rankine cycles for waste heat recovery: Application in an offshore platform. Energy, in press.

[5] Wang M, Wang J, Zhao Y, Zhao P, Dai Y. Thermodynamic analysis and optimization of a solar –driven regenerative organic Rankine cycle (ORC) based on flat-plate solar collectors. Applied Thermal Energy 2012;50:816-825.

[6] Lakew A, Bolland O, Working fluids for low-temperature heat source. Applied Thermal Energy 2010;30 :1262-1268.

[7] Wang J, Yan Z, Wang M, Li M, Dai Y, Multi-objective optimization of an organic Rankine cycle (ORC) for low grade waste heat recovery using evolutionary algorithm. Energy Conversion and Management 2013; 71:146-158.

[8] Liu B, Chien K, Wang C. Effect of working fluids on organic Rankine cycle for waste heat recovery. Energy 2004;29:1207-1217.

[9] The MathWorks, Inc., 2012, “General Release Notes for R2012a”.

[10] Lemmon, W.E., Huber, L.M., and McLinden, O.M., 2010, “NIST Reference Fluid Thermodynamic and Transport Properties-REFPROP, Version 9.0, User´s guide”, Thermophysical Properties Division, National Institute of Standards and Technology, Boulder, Colorado (USA).

[11] Kuo CR, Hsu SW, Chang KH, Wang CC. Analysis of a 50 kW organic Rankine cycle system. Energy 2011;36:5877-5885.

[12] Wei DH, Lu XS, Lu Z, Gu JM. Performance analysis and optimization of organic Rankine cycles (ORC) for waste heat recovery. Energy Conversion and Management 2007; 48: 1113-9.

[13] Ramesh K. Shah and Dušan P. Sekulic, Fundamentals of Heat Exchanger Design., 2003 John Wiley & Sons, Inc.

[14] J, M. Coulson and J. F. Richardson, Chemical Engineering, Volume 1, Sixth edition Fluid Flow, Heat Transfer and Mass Transfer.

[15] Ayub ZH. Plate Heat exchanger literature survey and new heat transfer and pressure drop correlations for refrigerant evaporators. Heat Transfer Engineering 2003; 24:3-16.

[16] Han DH, Lee KJ, Kim YH. Experiments on the characteristics of evaporation of R410A in brazed plate heat exchangers with different geometric configurations. Applied Thermal Engineering 2003;23:1209-1225.

[17] Longo G, Gasparella A, Sartori R. Experimental heat transfer coefficients during refrigerant vaporisation and condensation inside herringbone-type plate heat exchangers with enhanced surfaces. International Journal of Heat and Mass Transfer 2004; 47: 4125-4136.

[18] T. Kuppan, Heat exchanger design handbook, 2000, Marcel Dekker, Inc.